



## Article

# Constructing FeS and ZnS Heterojunction on N, S-Codoped Carbon as Robust Electrocatalyst toward Oxygen Reduction Reaction

Fenglai Pei <sup>1,†</sup>, Min Li <sup>2,†</sup>, Yifan Huang <sup>2</sup>, Qiuyun Guo <sup>3</sup>, Kunming Song <sup>3</sup>, Fantao Kong <sup>2,\*</sup> and Xiangzhi Cui <sup>2,3,\*</sup><sup>1</sup> Shanghai Motor Vehicle Inspection Certification & Tech Innovation Center Co., Ltd., Jiading District, Shanghai 201805, China; fenglaipei@smvic.com.cn<sup>2</sup> Shanghai Institute of Ceramics, Chinese Academy of Sciences, Shanghai 200050, China; limin232@mailsucas.ac.cn (M.L.); huangyifan231@mailsucas.ac.cn (Y.H.)<sup>3</sup> School of Chemistry and Materials Science, Hangzhou Institute for Advanced Study, University of Chinese Academy of Sciences, Hangzhou 310024, China; guoqiuyun22@mailsucas.ac.cn (Q.G.); songkunming22@mailsucas.ac.cn (K.S.)

\* Correspondence: kongfantao@mail.sic.ac.cn (F.K.); cuixz@mail.sic.ac.cn (X.C.)

† These authors contributed equally to this work.

## Electrochemical measurements

The ORR performance was evaluated on the standard three-electrode system connected with CHI 760E electrochemical workstation (CH Instruments, China) at room temperature. The glassy carbon electrode (GCE, 3 mm in diameter) coated with catalyst was used as working electrode. The ink of catalysts was prepared by dispersing 10 mg of the as-synthesized samples into 1 mL of isopropanol. Then, 30  $\mu$ L of 5 wt.% Nafion D-520 dispersion was added to the mixture and ultrasound for about 30 minutes. Subsequently, 15  $\mu$ L of the catalyst ink was dropped onto the surface of the glassy carbon electrode and then dried at room temperature before tests. The ink of Pt/C (20 wt.%) was also prepared by the same method. The loading of the as-prepared catalysts and Pt/C are 0.40 mg cm<sup>-2</sup> and 0.60 mg cm<sup>-2</sup> in alkaline and acidic electrolytes, respectively. The Ag/AgCl and carbon rod were used as reference electrode and counter electrodes, respectively. The Nernst equation ( $E_{\text{RHE}} = E_{\text{Ag/AgCl}} + 0.059 \times \text{pH} + 0.1989 \text{ V}$ ) was used to standardized all test potentials to reversible hydrogen electrode (vs. RHE).

The electrocatalytic performance of catalysts was evaluated in 0.1 M KOH or 0.5 M H<sub>2</sub>SO<sub>4</sub> electrolytes. Linear scanning voltammetry (LSV) curves were recorded by rotating disc electrode (RDE) techniques at a constant rotating speed of 1600 rpm in different electrolytes with the scan rate of 5 mV·s<sup>-1</sup>. The electron transfer number ( $n$ ) of ORR was calculated based on the Koutecky-Levich (K-L) equation:

$$\frac{1}{j} = \frac{1}{j_k} + \frac{1}{j_L} = \frac{1}{j_k} + \frac{1}{B\omega^{1/2}}$$

$$B = 0.62nFD_{\text{O}_2}^{2/3}v^{-1/6}C_0$$

$$j_k = \frac{j_L \times j}{j_L - j}$$

where  $j$  is the measured disk current density,  $j_L$  and  $j_k$  are the diffusion-limiting current densities and kinetic current densities, respectively.  $\omega$  is the electrode rotation rate (rad s<sup>-1</sup>).  $n$  is the number of electrons transferred per O<sub>2</sub> molecule.  $C_0$  is the oxygen concentration of electrolyte ( $1.2 \times 10^{-6}$  mol cm<sup>-3</sup>),  $D_{\text{O}_2}$  is the diffusion coefficient of O<sub>2</sub> ( $1.9 \times 10^{-5}$  cm<sup>2</sup>·s<sup>-1</sup>),  $v$  is the kinetic viscosity of the electrolyte, and  $F$  is Faraday constant (96485 C mol<sup>-1</sup>).

Next, the linear part of the Tafel curves was matched to the Tafel equation ( $\eta = a + b \log|j|$ ), and then the Tafel slope ( $b$ ) was obtained to evaluate the kinetic performance of

the as-prepared catalysts. The long-time stability was evaluated by chronoamperometry in alkaline and acidic media, respectively, with the electrode rotating speed of 1600 rpm.

Cyclic voltammetry (CV) tests were measured in N<sub>2</sub>/O<sub>2</sub>-saturated electrolytes with a sweep rate of 10 mV s<sup>-1</sup>. The electrochemically active surface area (ECSA) of the different catalysts was estimated from the electrochemical double layer capacitance (*C<sub>dl</sub>*) obtained from CV curves in a non-faradaic potential range (1.02–1.12 vs. RHE) at different scan rates (10–30 mV s<sup>-1</sup>). The ECSA can be calculated by the following equation:

$$ECSA = C_{dl} / C_s$$

Where the value of *C<sub>s</sub>* is usually 0.04 mF cm<sup>-2</sup> in alkaline electrolyte.

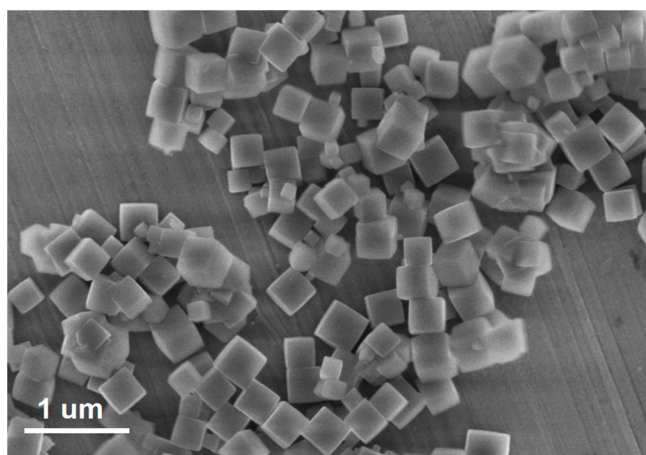


**Figure S1.** SEM image of ZIF-8.

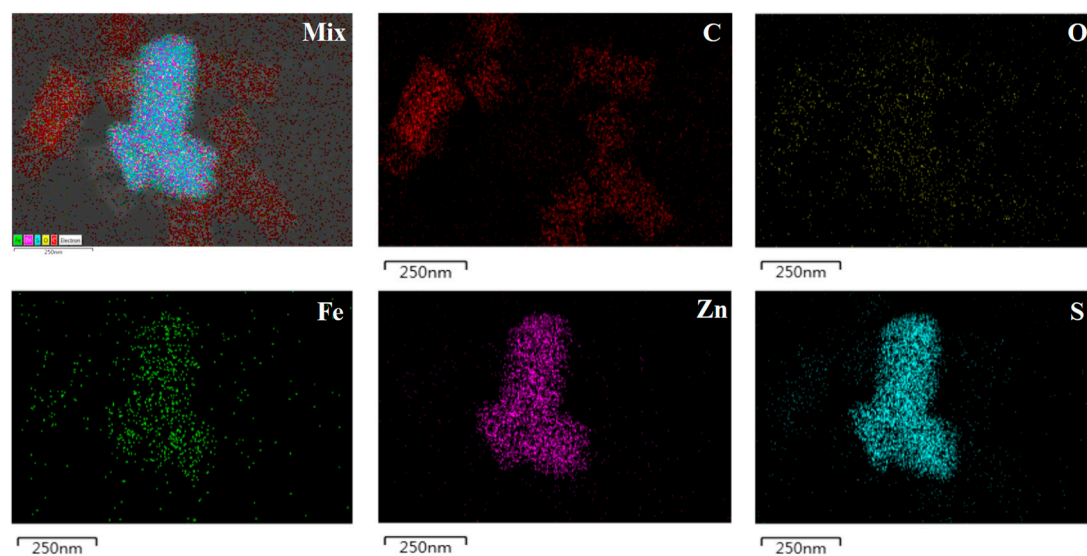


**Figure S2.** SEM image and element mapping of carbon, oxygen, sulfur, zinc and iron of Zn/Fe-SNC.

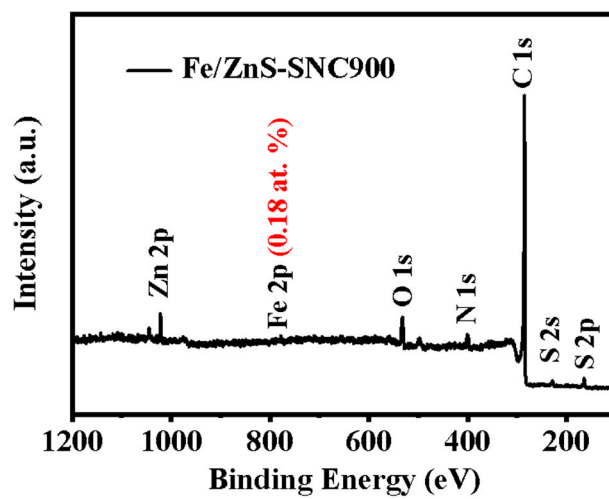


**Figure S3.** The survey XPS spectrum of Fe/ZnS-SNC900.

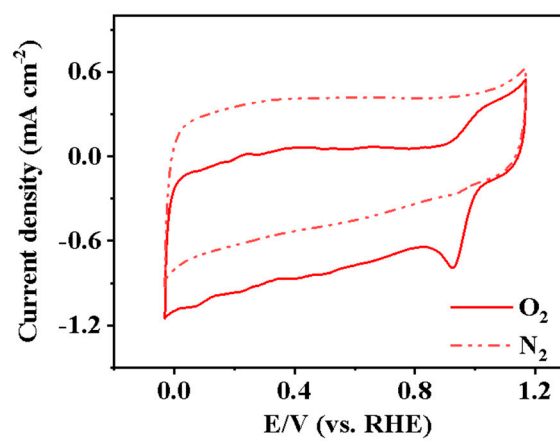


**Figure S4.** CV curves of Fe/ZnS-SNC900 in O<sub>2</sub>- or N<sub>2</sub>-saturated 0.1 M KOH solution.

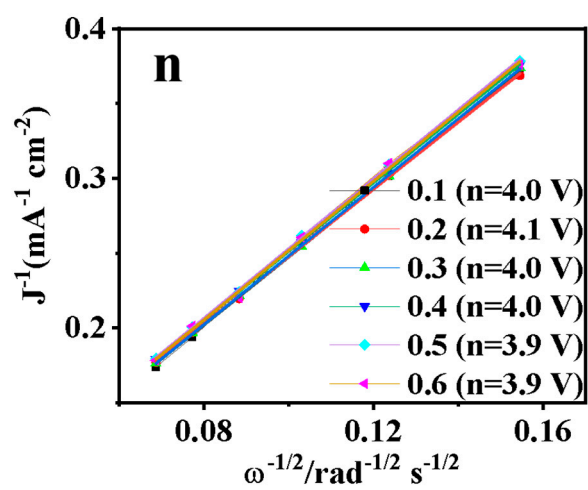
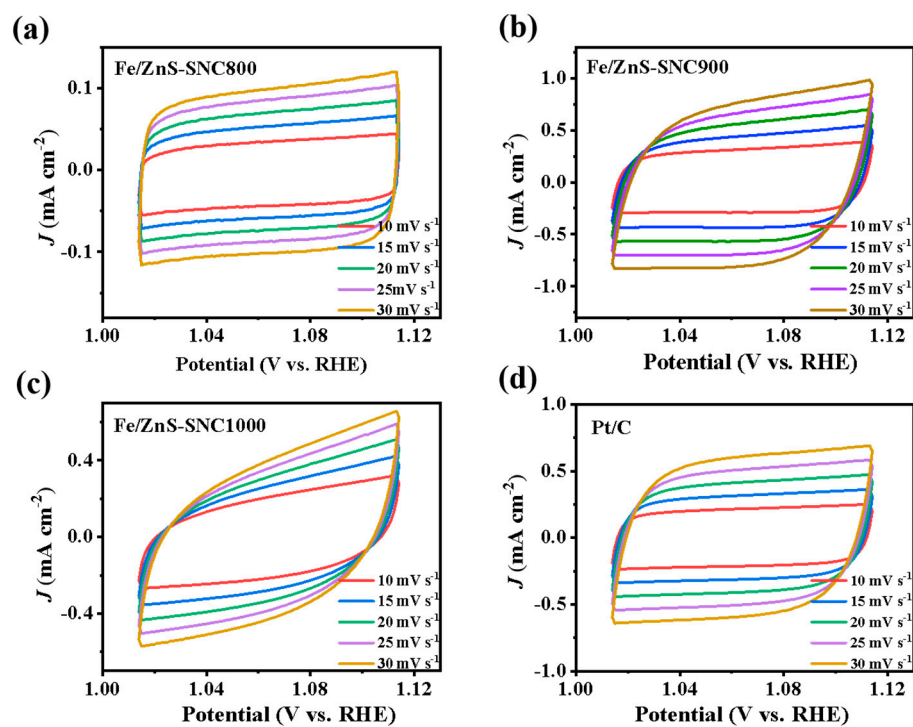


Figure S5. K-L plots of Fe/ZnS-SNC900 in 0.1 M KOH solution.



**Figure S6.** CV curves at various scan rates of Fe/ZnS-SNC800 (a), 900 (b), 1000 (c) and Pt/C (d) catalysts in the range of 1.02–1.12 V in 0.1 M KOH solution.

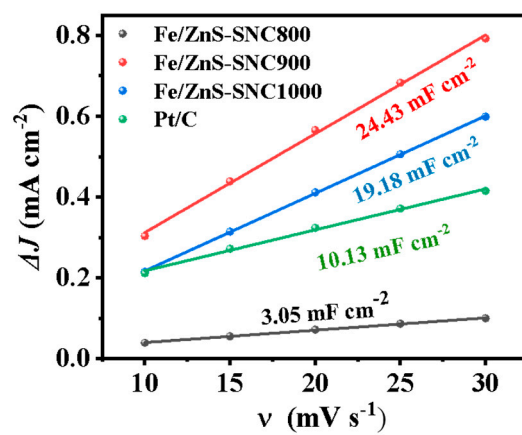
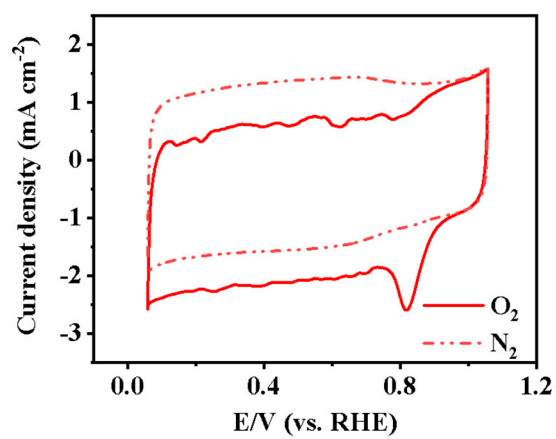


Figure S7. Double-layer capacitance  $C_{dl}$  of Fe/ZnS-SNC800, 900, 1000 and Pt/C catalysts.





**Figure S8.** CV curves of Fe/ZnS-SNC900 in O<sub>2</sub>- or N<sub>2</sub>-saturated 0.5 M H<sub>2</sub>SO<sub>4</sub> solution.

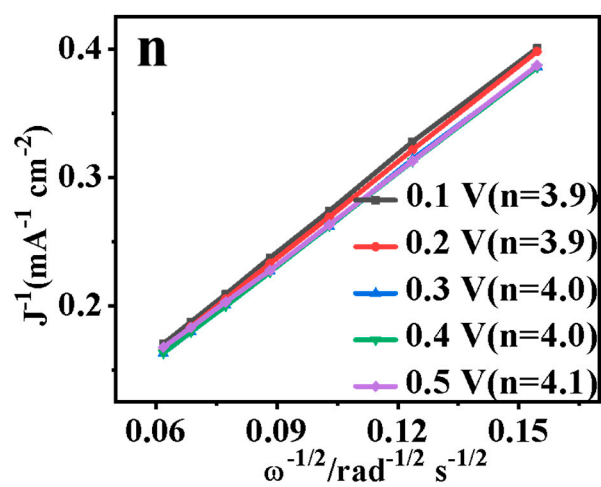
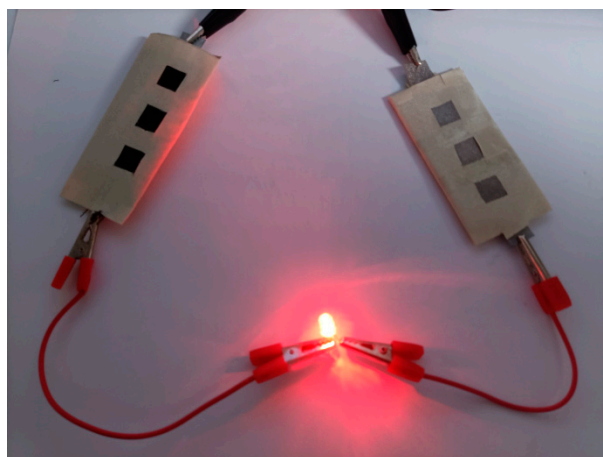


Figure S9. K-L plots of Fe/ZnS-SNC900 in 0.5 M H<sub>2</sub>SO<sub>4</sub> solution.



**Figure S10.** Photograph of a red light-emitting diode powered by two integrated sandwich-type ZABs in series.

**Table S1.** Comparison of ORR activities in alkaline electrolyte among Fe/ZnS-SNC and other non-noble metal electrocatalysts reported in the literature.

Catalysts	Electrolyte	$E_{\text{onset}}$ (V)	$E_{1/2}$ (V)	References
FeN <sub>4</sub> -Ten	0.1 M KOH	0.922	0.867	<i>Adv. Mater.</i> , 2022, 3, 2202714
(Zn, Cu)-NC	0.1 M KOH	~	0.880	<i>Adv. Funct. Mater.</i> , 2022, 32, 2203471
PtFeNC	0.1 M KOH	1.050	0.895	<i>Appl. Catal. B: Environ.</i> 2021, 286, 119891
Fe,Mn/N-C	0.1 M KOH	0.979	0.928	<i>Nat. Commun.</i> 2021, 12, 1734
Ru-SAS/SNC	0.1 M KOH	0.998	0.861	<i>J. Am. Chem. Soc.</i> 2022, 144, 2197-2207
Fe/Ni-N-C	0.1 M KOH	1.005	0.861	<i>Appl. Catal. B: Environ.</i> 2021, 285, 119778
Fe-N/P-C-700	0.1 M KOH	0.941	0.867	<i>J. Am. Chem. Soc.</i> 2020, 142, 2404
Fe, Co SAs-PNCF	0.1 M KOH	1.040	0.930	<i>Nano Energy</i> , 2022, 93, 106793
COF@MOF800	0.1 M KOH	0.830	0.730	<i>Small Structures</i> , 2022, 3, 2100225
FeN <sub>4</sub> -O-NCR	0.1 M KOH	1.05	0.940	<i>Energy Environ. Sci.</i> , 2022, 15, 2619-2628
Fe-SA/Meso-C	0.1 M KOH	~	0.926	<i>Carbon</i> , 2022, 191, 393-402
ZFP-800	0.1 M KOH	1.028	0.875	<i>J. Colloid Interf. Sci.</i> 2022, 608, 446-458
<b>Fe/ZnS-SNC</b>	<b>0.1 M KOH</b>	<b>1.080</b>	<b>0.938</b>	<b>This work</b>

**Table S2.** Comparison of the flexible ZAB performances using Fe/ZnS-SNC and other recently reported ORR electrocatalysts.

Catalyst	Open circuit voltage (V)	Peak power density (mW cm <sup>-2</sup> )	References
FeP/Fe <sub>2</sub> O <sub>3</sub> @NPCA	1.42	40.8	<i>Adv. Mater.</i> 2020, 32, 2002292
SAFe-SWCNT	1.36	33	<i>Appl. Catal. B: Environ.</i> 2021, 294, 120239
ODAC-CoO-30	1.41	42	<i>Adv. Funct. Mater.</i> 2021, 31, 2101239
FeCo/Se-CNT	1.41	37.5	<i>Nano Lett.</i> 2021, 21, 2255
SAFe-SWCNT	1.36	33	<i>Appl. Catal. B: Environ.</i> 2021, 294, 120239
FeNi <sub>3</sub> @NC	1.38	—	<i>Appl. Catal. B: Environ.</i> 2020, 268, 118729
ODAC-CoO-30	1.41	42	<i>Adv. Funct. Mater.</i> 2021, 31, 2101239
<b>Fe/ZnS-SNC</b>	<b>1.45</b>	<b>30.8</b>	<b>This work</b>